Saturation of Turbulent Helical Dynamos

Guillaume Bermudez, Alexandros Ens Alexakis

Saturation of Turbulent Helical Dynamos

Guillaume Bermudez and Alexandros Alexakis*
Laboratoire de Physique de l'Ecole Normale Supérieure, ENS, Université PSL, CNRS, Sorbonne Université, Université Paris Cité, F-75005 Paris, France
(Dated: Received 29 April, 2022; revised, 6 October 2022; accepted 18 October 2022)

The presence of large scale magnetic fields in nature is often attributed to the inverse cascade of magnetic helicity driven by turbulent helical dynamos. In this Letter we show that in turbulent helical dynamos, the inverse flux of magnetic helicity toward the large scales $\Pi_{\mathcal{H}}$ is bounded by $|\Pi_{\mathcal{H}}| \le c\epsilon k_\eta^{-1}$, where ϵ is the energy injection rate, k_η is the Kolmogorov magnetic dissipation wave number and c an order one constant. Assuming the classical isotropic turbulence scaling, the inverse flux of magnetic helicity $\Pi_{\mathcal{H}}$ decreases at least as a $-3/4$ power law with the magnetic Reynolds number Rm : $|\Pi_{\mathcal{H}}| \le c\epsilon\ell_f Rm^{-3/4}\max[Pm,1]^{1/4}$, where Pm the magnetic Prandtl number and ℓ_f the forcing lengthscale. We demonstrate this scaling with Rm using direct numerical simulations of turbulent dynamos forced at intermediate scales. The results further indicate that nonlinear saturation is achieved by a balance between the inverse cascade and dissipation at domain size scales L for which the saturation value of the magnetic energy is bounded by $\mathcal{E}_{\rm m} \le cL(\epsilon\ell_f)^{2/3}Rm^{1/4}\max[1,Pm]^{1/4}$. Numerical simulations also demonstrate this bound. These results are independent of the dynamo mechanism considered. In our setup, they imply that inviscid mechanisms cannot explain large scale magnetic fields and have critical implications for the modelling of astrophysical dynamos.

I. INTRODUCTION

Magnetic fields are observed in a plethora of astrophysical objects from planetary to galactic scales [1–3]. Their generation and sustainment is often attributed to dynamo action: their self-amplification by a continuous stretching and refolding of magnetic field lines due to the underlying (turbulent in most cases) flow [4, 5]. In many cases the magnetic structures formed span the entire astrophysical object, reaching scales much larger than the small scale turbulence that generates them. The pioneering work of [6] showed that large scale magnetic fields can be generated from small scale flows if the advecting flow is helical. This result is based on an expansion for large scale separation and is referred as "alpha dynamo." However, such expansion can be formally done only below a critical value of the magnetic Reynolds number Rm (the ratio of Ohmic to dynamic timescales). Above this critical value small scale dynamo action begins and the expansion ceases to be valid [7–9].

The validity of the alpha model is further questioned in the nonlinear regime for which the magnetic field feeds back to the velocity field through the Lorentz force. In [10, 11] it was argued that the growth of alpha dynamos saturates when the large scale magnetic field $\mathbf{B}$ becomes larger than $U_{\rm rms}Rm^{-1/2}$, where $U_{\rm rms}$ is the root mean square value of the velocity fluctuations. This gives a very weak magnetic field for most astrophysical applications for which $Rm \gg 1$. Two scale models have also been extensively used to predict saturation magnetic energy [12, 13] but their application is limited for large Rm where turbulence sets in.

An alternative way of explaining the formation of large magnetic fields is through the inverse cascade of magnetic helicity [14, 15]. This intrinsically nonlinear mechanism (which is, however, compatible with alpha dynamos) predicts that magnetic helicity will be transferred by nonlinear interactions to larger scales. Indeed, several works that followed [16–21] demonstrated with numerical simulations that when magnetic helicity is injected in a flow (by a dynamo or other mechanism), it cascades inversely to larger scales. The values of Rm examined ranged from few times the small scale dynamo onset $Rm_{\rm c} \simeq 10$ [16–19] to much larger [20, 21]. However, to our knowledge, the dependence of the inverse cascade of magnetic helicity on Rm has not been tested before. A quantitative understanding of how turbulent helical dynamos saturate with clear predictions on the saturating amplitude does not exist.

In this Letter we demonstrate by analytical arguments and numerical simulations that in dynamo flows, the inverse cascade of magnetic helicity is bounded from above by a decreasing power of Rm. Thus it cannot survive the infinite Rm limit. This leads to a prediction for the saturation amplitude of the magnetic field that we test with numerical simulations.

II. THEORETICAL ARGUMENTS

We begin by considering the magnetohydrodynamics (MHD) equations for the incompressible velocity $\mathbf{u}$ and magnetic field $\mathbf{b}$ given by

$$\partial_t\mathbf{u} + \mathbf{u}\cdot\nabla\mathbf{u} = -\nabla P + (\nabla\times\mathbf{b})\times\mathbf{b} + \nu\nabla^2\mathbf{u} + \mathbf{f}, \quad (1)$$

$$\partial_t\mathbf{b} = \nabla\times(\mathbf{u}\times\mathbf{b}) + \eta\nabla^2\mathbf{b}, \quad (2)$$

in a cubic periodic domain of size $2\pi L$, with ν being the viscosity, η the magnetic diffusivity, P the pressure, and $\mathbf{f}$ an external mechanical force. In absence of viscous and Ohmic dissipation, and external forcing, the total energy $\mathcal{E} = \frac{1}{2}\langle|\mathbf{u}|^2+|\mathbf{b}|^2\rangle$ and magnetic helicity $\mathcal{H} = \frac{1}{2}\langle\mathbf{a}\cdot\mathbf{b}\rangle$ are

* alexakis@phys.ens.fr

conserved ; here the angular brackets stand for spatial integration and $\mathbf{a} = -\nabla^{-2}\nabla\times\mathbf{b}$ is the vector potential. Their balance reads

$$\partial_t \mathcal{E} = \mathcal{I}_\mathcal{E} - \epsilon, \qquad \partial_t \mathcal{H} = -\epsilon_\mathcal{H}, \tag{3}$$

where $\mathcal{I}_\mathcal{E} = \langle \mathbf{f}\cdot\mathbf{u}\rangle$ is the energy injection rate, $\epsilon = \epsilon_u + \epsilon_b$ is the energy dissipation rate with $\epsilon_u = \nu\langle|\nabla\mathbf{u}|^2\rangle$ the viscous dissipation rate and $\epsilon_b = \eta\langle|\nabla\mathbf{b}|^2\rangle$ the Ohmic dissipation rate. Finally $\epsilon_\mathcal{H} = \eta\langle\mathbf{b}\cdot\nabla\times\mathbf{b}\rangle$ is the helicity generation or dissipation rate. The forcing $\mathbf{f}$ is assumed to act on a scale $\ell_f = k_f^{-1} \ll L$ while dissipation acts at the smaller viscous scale ℓ_ν and Ohmic scale ℓ_η. For large Reynolds number $Re = \epsilon^{1/3}\ell_f^{4/3}/\nu$ and large magnetic Reynolds number $Rm = \epsilon^{1/3}\ell_f^{4/3}/\eta$, the dissipation length scales ℓ_ν, ℓ_η scale like [22]

$$\ell_\nu \propto \ell_f Re^{-3/4} \quad \text{and} \quad \ell_\eta \propto \ell_f Rm^{-3/4} \tag{4}$$

for $Pm \le 1$ while for $Pm \ge 1$

$$\ell_\nu \propto \ell_f Re^{-3/4} \quad \text{and} \quad \ell_\eta \propto \ell_f Rm^{-3/4} Pm^{1/4}, \tag{5}$$

where $Pm = \nu/\eta$ is the magnetic Prandtl number.

At intermediate scales ℓ (so-called inertial scales $\ell_f \ll \ell \ll \ell_\eta, \ell_\nu$), there is a constant flux of energy across scales given by

$$\Pi_\mathcal{E}(k) = \langle \mathbf{u}_k^< \cdot (\mathbf{u}\cdot\nabla\mathbf{u} - \mathbf{b}\cdot\nabla\mathbf{b}) - \mathbf{b}_k^< \cdot (\nabla\times\mathbf{u}\times\mathbf{b})\rangle, \tag{6}$$

where $\mathbf{u}_k^<, \mathbf{b}_k^<$ stand for the filtered velocity and magnetic field, respectively, so that only Fourier modes with wave numbers of norm smaller than $k = 1/\ell$ are kept [23]. Conservation of energy by the nonlinear terms implies that the energy flux at the inertial scales is constant in k and equals the energy dissipation rate $\Pi_\mathcal{E}(k) = \epsilon$.

Similarly, there is a flux of magnetic helicity [18]

$$\Pi_\mathcal{H}(k) = -\langle \mathbf{b}_\mathbf{k}^< \cdot (\mathbf{u}\times\mathbf{b})\rangle \tag{7}$$

that also has to be constant at scales in which dissipation plays no role. However, unlike energy, the forcing does not inject magnetic helicity which can be only generated or destroyed by the Ohmic dissipation at rate $\epsilon_\mathcal{H}$. Nonetheless if the forcing is helical the flow can transport magnetic helicity from the small Ohmic scales to ever larger scale $L' > \ell_f$ up until the domain size reached $L' \simeq L$ where a helical condensate will form. Conservation of magnetic helicity by the nonlinear terms implies again that the flux of helicity at scales $L' \gg \ell \gg \ell_\eta$ has to be constant in $k \propto 1/\ell$ with $\Pi_\mathcal{H}(k) = \epsilon_\mathcal{H}$.

The two cascades, energy and helicity, are not independent and the first limits the latter [24]. To show that, we write the magnetic field in Fourier space $\tilde{\mathbf{b}}_\mathbf{k}$ using the helical basis $\tilde{\mathbf{b}}_\mathbf{k} = b_\mathbf{k}^+\mathbf{h}_\mathbf{k}^+ + b_\mathbf{k}^-\mathbf{h}_\mathbf{k}^-$ where

$$\mathbf{h}_\mathbf{k}^\pm = \frac{1}{\sqrt{2}}\frac{\mathbf{k}\times(\mathbf{k}\times\mathbf{e})}{|\mathbf{k}\times(\mathbf{k}\times\mathbf{e})|} \pm \frac{i}{\sqrt{2}}\frac{\mathbf{k}\times\mathbf{e}}{|\mathbf{k}\times\mathbf{e}|} \tag{8}$$

are the eigenvectors of the curl operator with $\mathbf{e}$ an arbitrary vector (non-parallel to $\mathbf{k}$) [25, 26]. By doing that we can write the magnetic energy spectrum as $E_b(k) = E_b^+(k) + E_b^-(k)$ and the magnetic helicity spectrum as $H(k) = (E_b^+(k) - E_b^-(k))/k$ where $E_b^\pm(k)\mathrm{d}k = \sum_{k\le|\mathbf{k}|<k+\mathrm{d}k}|b_\mathbf{k}^\pm|^2$ is the sum of the energy of the $b^\pm$ Fourier modes on a spherical shell of width $\mathrm{d}k$ and radius k. Since magnetic helicity is primarily generated at Ohmic wave numbers $k_\eta = 1/\ell_\eta$ for any wave number k in the range $k \le k_\eta$ we can write

$$\begin{aligned}|\Pi_\mathcal{H}(k)| &= |\epsilon_\mathcal{H}| \\ &\simeq \eta\left|\int_k^\infty q[E_b^+(q) - E_b^-(q)]\mathrm{d}q\right| \\ &\le \eta k^{-1}\int_k^\infty q^2\left|E_b^+(q) + E_b^-(q)\right|\mathrm{d}q \\ &= k^{-1}\epsilon_b\end{aligned} \tag{9}$$

This result holds for any k in the inertial range. Choosing $k = k_\eta/c$, where $c > 1$ is an order one constant, and using $\epsilon_b \le \epsilon$, we obtain our final result

$$|\Pi_\mathcal{H}(k)| \le c\,\epsilon/k_\eta. \tag{10}$$

In other words the maximum possible value of $|\epsilon_\mathcal{H}|$ is obtained if all magnetic energy at Ohmic scales k_η^{-1} is concentrated at only positive or only negative helicity modes, in which case $|\epsilon_\mathcal{H}| = \epsilon_b/k_\eta$. Thus the flux of magnetic helicity is bounded by the energy injection rate divided by the Ohmic dissipation wave number k_η. Note that this bound is saturated if the magnetic field at small scales is fully helical. If not, $|\Pi_\mathcal{H}|$ can be much smaller than (10). Using the estimates for k_η for isotropic MHD turbulence we obtain

$$|\Pi_\mathcal{H}(k)| \le c\epsilon k_f^{-1} Rm^{-3/4}\max[1, Pm]^{1/4}, \tag{11}$$

where c is an order one constant. Given the very large values of Rm in nature this gives very little hope of observing such fluxes.

However, despite having a diminishing flux of magnetic helicity for large Rm, this does not mean that large scale dynamos cannot be observed. In a finite domain of size L a magnetic helicity condensate will form. Its magnetic field amplitude B will be determined by a balance of magnetic helicity flux with the magnetic helicity dissipation at that scale so that $\Pi_\mathcal{H} \propto \eta B^2/L$. Using the previous estimate for the flux leads to the prediction for the large scale energy $\mathcal{E}_m = B^2$ given by

$$\mathcal{E}_m \le c\,\epsilon^{2/3} L k_f^{1/3} Rm^{1/4}\max[1, Pm]^{1/4}. \tag{12}$$

We note that a very long time $T \sim (B^2 L)/\Pi_\mathcal{H} \propto Rm$ would be required for such a field to be formed. Furthermore if there is an other η-independent mechanism for magnetic helicity saturation, like magnetic helicity expulsion [27, 28], then the amplitude of the large scale magnetic field will diminish to zero as $Rm \to \infty$.

Finally we note that this result is based on strong turbulence scaling of k_η. One can argue that as the

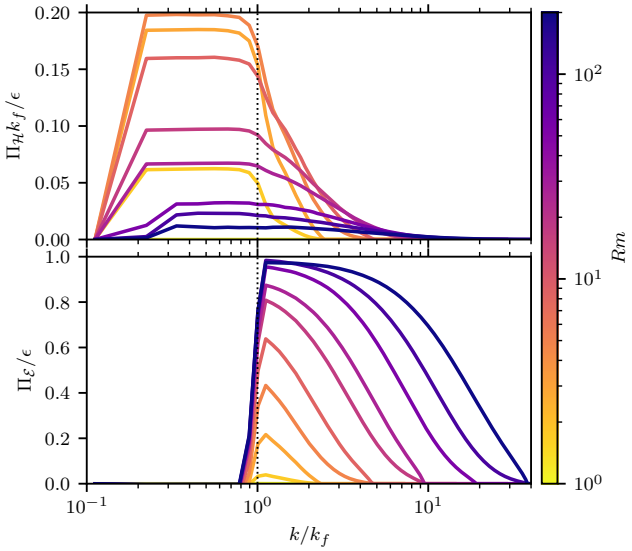

FIG. 1. Magnetic helicity flux $\Pi_{\mathcal{H}}$ (top) and total energy flux $\Pi_{\mathcal{E}}$ (bottom) for several values of the magnetic Reynolds number Rm for $k_f L = 8$.

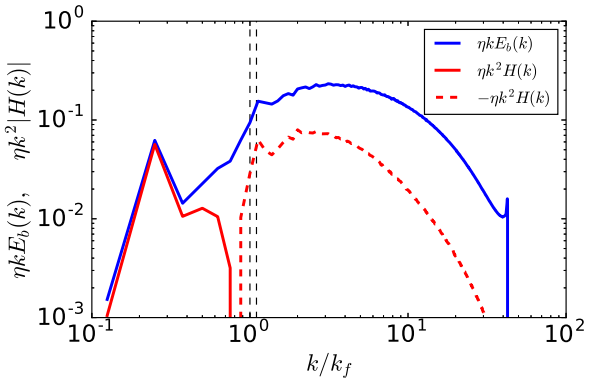

FIG. 2. Magnetic helicity dissipation/generation spectrum $\eta k^2 H(k)$ and normalized magnetic energy spectrum $\eta k E_b(k)$ for the case with hypodissipation with $k_f L = 8$ and the largest attained magnetic Reynolds number Rm.

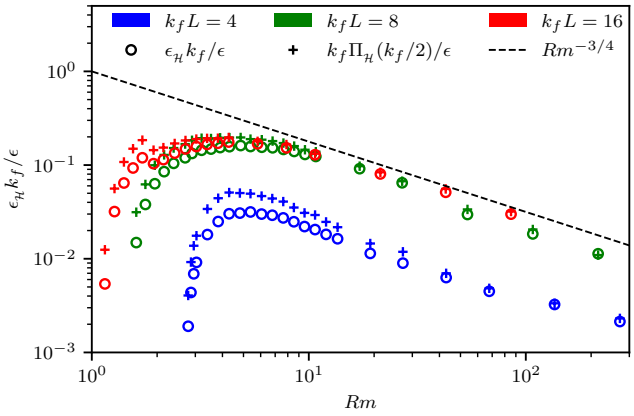

FIG. 3. Magnetic helicity generation rate $\epsilon_{\mathcal{H}}$ (circles) and magnetic flux $\Pi_{\mathcal{H}}(k_f/2)$ (crosses) as a function of the magnetic Reynolds number Rm for three different values of $k_f L = 4$ (blue), $k_f L = 8$ (green) and $k_f L = 16$ (red).

large scale magnetic field builds up the relation between k_η and Rm can change from that of strong turbulence to that of weak turbulence [29] or turbulence driven by the large scale magnetic shear [30]. Both of these options lead to a faster increase of $\mathcal{E}_m$ with Rm as $\mathcal{E}_m \lesssim c\,\epsilon^{2/3} L^{5/6} k_f^{-8/15} Rm^{2/5}$ that is not found, however, in the numerical studies that follow.

III. NUMERICAL SIMULATIONS

To demonstrate the above arguments we perform a series of numerical simulations that solve the MHD equations (1–2) using the pseudospectral code GHOST [31] in a cubic domain of side $2\pi L$ with a fully helical random delta correlated forcing at wave number $k_f = 1/\ell_f$ that fixes the energy injection rate ϵ. The magnetic Prandtl number $Pm = \nu/\eta$ was set to unity for all runs. The resolution used varied from 128^3 grid points to 1024^3 grid points for the largest Rm. The resolution was chosen so that the largest inertial range is obtained while remaining well resolved with a clear dissipation wave number range. All measurements were obtained by time averaging at steady state.

As a first step to accommodate for the large scale pile up of magnetic helicity we introduce a magnetic hypodissipation term $\eta_h \nabla^{-2}\mathbf{b}$ in (2) that arrests large scale magnetic helicity. With the inclusion of this term, the simulations quickly reach a steady state where the helicity generated at the small scales by $\epsilon_{\mathcal{H}}$ is transported and dissipated at the largest scales by hypodissipation.

Figure 1 shows the magnetic helicity flux (top) and energy flux (bottom) for a series of runs varying Rm as shown in the legend for $k_f L = 8$. The energy flux shows its classical behavior increasing as Rm is increased, approaching its maximal value $\Pi_{\mathcal{E}} \sim \epsilon$ in the inertial range. On the other hand, $\Pi_{\mathcal{H}}(k)$ first starts to increase with Rm once the dynamo onset is crossed (and magnetic energy and helicity appear in the system), reaches a maximum and then starts to decrease again when the cascades builds up so that the constrain in (10) becomes relevant.

The magnetic helicity generation spectrum $\eta k^2 H(k)$ for the largest Rm is shown in Fig. 2. The solid line corresponds to positive values of $\eta k^2 H(k)$ while the dashed line corresponds to negative values of $\eta k^2 H(k)$; thus, negative magnetic helicity is generated at the smallest scales. In the same plot we show the normalized magnetic energy spectrum $\eta k E_b(k)$ that bounds $\eta k^2 |H(k)| \leq \eta k E_b(k)$ with the equality corresponding to a fully helical magnetic field.

The dependence of the magnetic helicity cascade with Rm is best seen in Fig. 3 where the magnetic helicity generation rate $\epsilon_{\mathcal{H}} k_f/\epsilon$ (circles) and the magnetic helicity

flux $\Pi_{\mathcal{H}}(k)$ at $k = k_f/2$ (crosses) are plotted as a function of Rm for three different scale separations $k_f L = 4, 8, 16$ in a log-log plot. All series show an initial increase of $\epsilon_{\mathcal{H}}$ and $\Pi_{\mathcal{H}}(k_f/2)$ followed afterward by a power law decrease with $\epsilon_{\mathcal{H}} \simeq \Pi_{\mathcal{H}}(k_f/2)$. The dashed lines give the predicted scaling $Rm^{-3/4}$ that appears to fit very well the observed power, verifying our prediction in Eq. (11).

A second series of numerical simulations with $k_f L = 8$ were performed without the hypoviscous term. The simulations were run for very long times until a steady state was reached such that magnetic energy did not increase further. The timescale to reach saturation is very long and this has limited us to using grids of size up to 512^3 and values of Rm 4 times smaller than the case with hypodissipation. Figure 4 shows with a red line the magnetic helicity dissipation spectrum $\eta k^2 H(k)$ for the largest Rm examined for these runs. Positive magnetic helicity is concentrated in a large scale condensate at $k = 1/L = k_f/8$ while it is negative for all smaller scales. As in Fig. 2 we also show $\eta k E_b(k)$ with a blue line. Note that while the large scales are fully helical small scales are less. The amplitude of the large scale condensate (at the smallest $k = k_f/8$) is so large that despite the small value of η the negative magnetic helicity generated at small scales by Ohmic diffusion is balanced by the positive helicity generated at the largest scale again by Ohmic diffusion. This leads to the flux of (negative) helicity from small to large scales shown in the lower panel of the same figure.

The balance between the magnetic helicity generated at small scales and dissipated at the large leads to the prediction (12) of a weak power law increase of magnetic energy $\mathcal{E}_m$ with Rm. Figure 5 shows $\mathcal{E}_m$ as a function of Rm in a log-log plot. The last three points appear to agree with the predicted power law. The range of values of Rm compatible with this law is, however, rather limited and smaller power laws or logarithmic increases cannot be excluded. In the inset of the same figure we show the same data in a lin-log plot demonstrating that the data could also be fitted to a logarithmic increase. A logarithmic increase, if true, is still compatible with the bound (12) but does not saturate it, and would imply that small scales become less and less helical as Rm is increased.

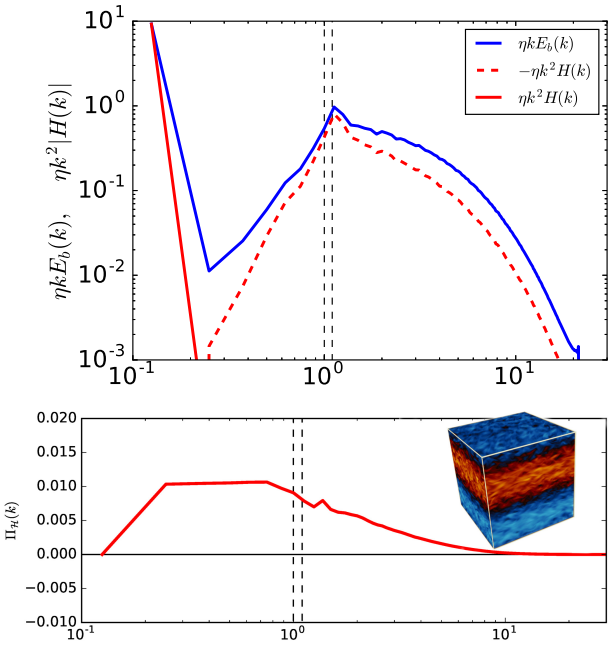

FIG. 4. Top panel: Magnetic helicity dissipation or generation spectrum $\eta k^2 H(k)$ and normalized magnetic energy spectrum $\eta k E_b(k)$ for the runs with no hypodissipation, with $k_f L = 8$, and the largest attained magnetic Reynolds number Rm. Bottom panel: magnetic helicity flux for the same run. The inset shows a visualization of the y-component of the magnetic field for this run.

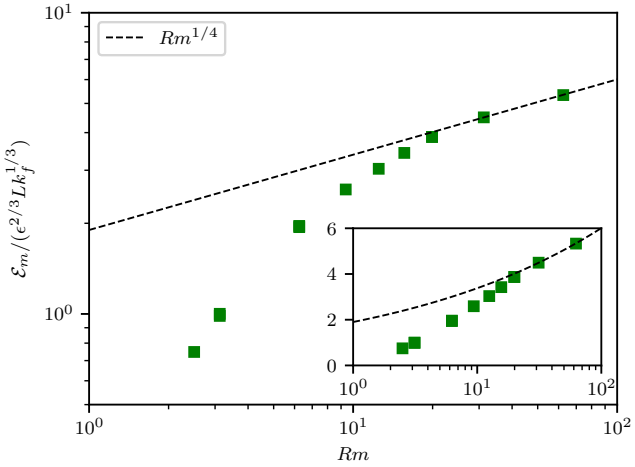

FIG. 5. Saturation of the magnetic energy $\mathcal{E}_{m,\mathrm{sat}}$ as a function of the magnetic Reynolds number Rm for $k_f L = 8$ in a log-log plot. The dashed line gives the prediction $Rm^{1/4}$. Inset: same figure in lin-log plot.

IV. CONCLUSION

This Letter gives for the first time estimates for the flux of magnetic helicity and the saturation of the magnetic field for the nonlinear state of a large Rm turbulent helical dynamo. Remarkably, even for asymptotically large values of Rm it has been shown that the magnetic helicity flux still depends on Rm and in fact it has to decrease at least as fast as $\Pi_{\mathcal{H}} \leq \epsilon/k_\eta \sim \epsilon/k_f Rm^{-3/4}$. This analytical result has also been clearly demonstrated by numerical simulations that are shown to follow this upper bound scaling. Furthermore it was shown that saturation is achieved by a balance of the inverse magnetic helicity flux with the helicity dissipation at the condensate scale. This has led to the prediction that the magnetic field amplitude at steady state is smaller than $Rm^{1/4}$. Numerical simulations are compatible with this result although the covered range of Rm cannot exclude other small power laws or logarithmic increases with Rm. It is important

to note that these results are based on magnetic helicity conservation and are independent of the actual dynamo mechanism involved (alpha or other). They are thus rather general. Therefore our work excludes any inviscid nonlinear theory for large scale dynamos from being realized. This means that any theory or model that attempts to explain the origin and amplitude of large scale magnetic fields should depend explicitly on resistivity, or find a way to circumvent the limitations imposed by our work by some other mechanism.

Such a circumvention can occur by magnetic helicity injection or expulsion through boundaries because our results were demonstrated and apply in closed periodic domains. In open domains like stars magnetic helicity can be expelled (or injected) through boundaries. Then magnetic helicity at large scales can saturate by expulsion and not Ohmic dissipation. In that case however we expect that the large scale magnetic field will be reduced to zero as $Rm \to \infty$. This conjecture however needs to be verified by future research.

The present results have critical implications for large magnetic fields in astrophysical systems and their origin because the basic understanding of the physical mechanisms involved and their estimates are put in question. As such the parametrisation of stellar and solar evolution models needs to be re-examined.

ACKNOWLEDGMENTS

This work was granted access to the HPC resources of MesoPSL financed by the Région Île-de-France and the project EquipMeso (project no. ANR-10-EQPX-29-01) and of GENCI-TGCC & GENCI-CINES (projects no. A0090506421 and no. A0110506421). This work been supported by the project Dysturb (project no. ANR-17-CE30-0004) financed by the Agence Nationale pour la Recherche (ANR).

[1] E. Falgarone and T. Passot, *Turbulence and magnetic fields in astrophysics*, Vol. 614 (Springer, 2008).
[2] A. Ruzmaikin, D. Sokoloff, and A. Shukurov, *Magnetic Fields of Galaxies*, Astrophysics and Space Science Library (Springer Netherlands, 1988).
[3] E. N. Parker, *Cosmical magnetic fields: Their origin and their activity* (Oxford university press, 1979).
[4] H. K. Moffatt, *Field generation in electrically conducting fluids*, Vol. 2 (1978).
[5] F. Rincon, Dynamo theories, Journal of Plasma Physics **85** (2019).
[6] M. Steenbeck, F. Krause, and K.-H. Rädler, Berechnung der mittleren lorentz-feldstärke für ein elektrisch leitendes medium in turbulenter, durch coriolis-kräfte beeinflußter bewegung, Zeitschrift für Naturforschung A **21**, 369 (1966).
[7] S. Boldyrev, F. Cattaneo, and R. Rosner, Magnetic-field generation in helical turbulence, Physical review letters **95**, 255001 (2005).
[8] F. Cattaneo and D. Hughes, Problems with kinematic mean field electrodynamics at high magnetic reynolds numbers, Monthly Notices of the Royal Astronomical Society: Letters **395**, L48 (2009).
[9] A. Cameron and A. Alexakis, Fate of alpha dynamos at large r m, Physical review letters **117**, 205101 (2016).
[10] S. I. Vainshtein and F. Cattaneo, Nonlinear restrictions on dynamo action, The Astrophysical Journal **393**, 165 (1992).
[11] D. Hughes, The mean electromotive force at high magnetic reynolds numbers, Plasma Physics and Controlled Fusion **50**, 124021 (2008).
[12] E. G. Blackman and G. B. Field, New dynamical mean-field dynamo theory and closure approach, Physical Review Letters **89**, 265007 (2002).
[13] E. G. Blackman, Recent developments in magnetic dynamo theory, Turbulence and Magnetic Fields in Astrophysics , 432 (2003).
[14] U. Frisch, A. Pouquet, J. Léorat, and A. Mazure, Possibility of an inverse cascade of magnetic helicity in magnetohydrodynamic turbulence, Journal of Fluid Mechanics **68**, 769 (1975).
[15] A. Pouquet, U. Frisch, and J. Léorat, Strong mhd helical turbulence and the nonlinear dynamo effect, Journal of Fluid Mechanics **77**, 321 (1976).
[16] A. Pouquet and G. Patterson, Numerical simulation of helical magnetohydrodynamic turbulence, Journal of Fluid Mechanics **85**, 305 (1978).
[17] A. Brandenburg, The inverse cascade and nonlinear alpha-effect in simulations of isotropic helical hydromagnetic turbulence, The Astrophysical Journal **550**, 824 (2001).
[18] A. Alexakis, P. D. Mininni, and A. Pouquet, On the inverse cascade of magnetic helicity, The Astrophysical Journal **640**, 335 (2006).
[19] W.-C. Müller, S. K. Malapaka, and A. Busse, Inverse cascade of magnetic helicity in magnetohydrodynamic turbulence, Physical Review E **85**, 015302 (2012).
[20] P. Bhat, K. Subramanian, and A. Brandenburg, A unified large/small-scale dynamo in helical turbulence, Monthly Notices of the Royal Astronomical Society **461**, 240 (2016).
[21] P. Bhat, K. Subramanian, and A. Brandenburg, Efficient quasi-kinematic large-scale dynamo as the small-scale dynamo saturates, arXiv preprint arXiv:1905.08278 (2019).
[22] A. A. Schekochihin, S. A. Boldyrev, and R. M. Kulsrud, Spectra and growth rates of fluctuating magnetic fields in the kinematic dynamo theory with large magnetic prandtl numbers, The Astrophysical Journal **567**, 828 (2002).
[23] D. Biskamp, *Magnetohydrodynamic turbulence* (Cambridge University Press, 2003).
[24] A. Alexakis and L. Biferale, Cascades and transitions in turbulent flows, Physics Reports **767**, 1 (2018).
[25] F. Waleffe, The nature of triad interactions in homogeneous turbulence, Physics of Fluids A: Fluid Dynamics **4**, 350 (1992).
[26] M. Linkmann, A. Berera, M. McKay, and J. Jäger, Helical mode interactions and spectral transfer processes in

magnetohydrodynamic turbulence, Journal of Fluid Mechanics **791**, 61 (2016).

[27] F. Rincon, Helical turbulent nonlinear dynamo at large magnetic reynolds numbers, Physical Review Fluids **6**, L121701 (2021).

[28] F. Cattaneo, G. Bodo, and S. Tobias, On magnetic helicity generation and transport in a nonlinear dynamo driven by a helical flow, Journal of Plasma Physics **86** (2020).

[29] S. Galtier, S. Nazarenko, A. C. Newell, and A. Pouquet, A weak turbulence theory for incompressible magnetohydrodynamics, Journal of plasma physics **63**, 447 (2000).

[30] A. Alexakis, Large-scale magnetic fields in magnetohydrodynamic turbulence, Physical Review Letters **110**, 084502 (2013).

[31] P. D. Mininni, D. Rosenberg, R. Reddy, and A. Pouquet, A hybrid mpi–openmp scheme for scalable parallel pseudospectral computations for fluid turbulence, Parallel computing **37**, 316 (2011).